Dalton Transactions

Accepted Manuscript

ROYAL SOCIETY OF CHEMISTRY

www.rsc.org/dalton

Graphical TOC

A modular approach for molecular recognition by zinc dipicolinate complexes

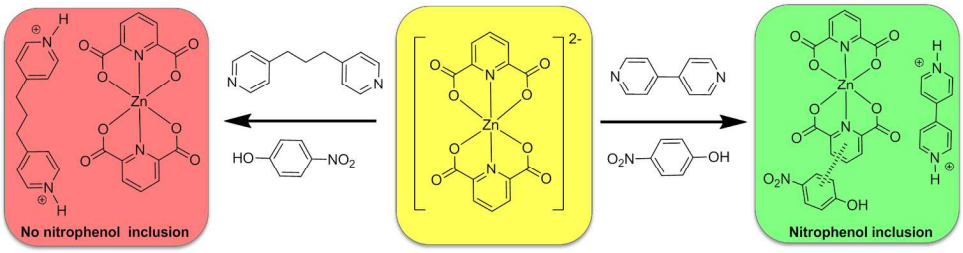

Recognition of 4-nitrophenol guest molecules by stacking and H-bonding interactions with 4,4′-bipyridinium zinc dipicolinate host was found and investigated in detail.

K. Shankar, A. M. Kirillov and J. B. Baruah*

A modular approach for molecular recognition by zinc dipicolinate complexes

Krapa Shankar[†], Alexander M. Kirillov[‡] and Jubaraj B. Baruah*[,†]

[†] Department of Chemistry, Indian Institute of Technology Guwahati, Guwahati 781 039 Assam, India,

Fax: + 91-361-2690762; Ph. + 91-361-2582311;

email: juba@iitg.ernet.in; Url: http://www.iitg.ac.in/juba

[‡]Centro de Química Estrutural, Complexo I, Instituto Superior Técnico, Universidade de Lisboa, Av. Rovisco Pais, 1049-001, Lisbon, Portugal.

Abstract

A series of zinc dipicolinate (2,6-pyridinedicarboxylate; pdc) complexes $[H_2tmbpy][Zn(pdc)_2]\cdot 5H_2O$ (**1**) {H_2tmbpy = 1,3-bis(4-pyridinium)propane(2+)}, $[H_2bpy][Zn(pdc)_2]\cdot 6H_2O$ (**2**) {H_2bpy = 4,4'-bipyridinium(2+)}, $[H_2bpy][Zn(pdc)_2]\cdot 3.5(4np)\cdot 2H_2O$ (**3**) {4np = 4-nitrophenol}, $[H_2tmbpy][Zn(pdc)_2]\cdot 4(2,7dhn)\cdot 3H_2O$ (**4**) {2,7dhn = 2,7-dihydroxynapthalene}, $[H_2bpy][Zn(pdc)_2]\cdot 2(2,7dhn)\cdot 5H_2O$ (**5**), $[H_2bpy][Zn(pdc)_2]\cdot 2(pyrogl)\cdot 6H_2O$ (**6**) {pyrogl = pyrogallol}, and $[H_2tmbpy][Zn(pdc)_2]\cdot 2(2,6dhn)\cdot 8H_2O$ (**7**) {2,6dhn = 2,6-dihydroxynapthalene} were synthesized and characterised. Different packing patterns in these complexes arise from differences in the ability of cations to π-stack with zinc dipicolinate units. In **2**, the planar $[H_2bpy]^{2+}$ moieties are *π*-stacked with adjacent 4,4'-bipyridinium cations and $[Zn(pdc)_2]^{2-}$ anions, whereas in **1** π-stacks are formed exclusively between $[Zn(pdc)_2]^{2-}$ moieties. 4-nitrophenol can selectively replace the $[H_2bpy]^{2+}$ cations to form an adduct **3**, thus representing a novel host-guest system for molecular recognition of 4-nitrophenol. This recognition does not occur upon treatment of 4-nitrophenol with **1** that bears a nonplanar $[H_2tmbpy]^{2+}$ cation. Host-guest interactions of pyrogallol, 2,6-dihydroxynaphthalene, and 2,7-dihydroxynapthalene with the parent complexes **1** and **2** were studied, resulting in the crystallization of **4–7.** Crystal structures of 5–**7** show that guest organic molecules are accommodated in the layers of zinc dipicolinate anions. The formation of different water clusters is also discussed. Besides, the topological analysis and classification of H-bonded patterns driven by strong hydrogen bonds between the

$[H_2bpy]^{2+}$ or $[H_2tmbpy]^{2+}$ cations and $[Zn(pdc)_2]^{2-}$ anions, and organic guest molecules was carried out. This analysis revealed: (i) the discrete 0D dimeric (in **1** and **2**) or tetrameric (in **7**) motifs with the 1M2-1 or 1,3M4-1 topology, respectively, (ii) the infinite 1D zigzag chains with the 2C1 topology in **5**, and (iii) the infinite 2D layers with the SP 2-periodic net (4,4)Ia and hcb [Shubnikov hexagonal plane net/(6,3)] topology in **6**, respectively.

Introduction

Soft supramolecular frameworks assembled from anionic species stabilized by charge-assisted hydrogen bonds generally show high stability and are useful in guest inclusion.[1] They have advantages to provide better flexibility than conventional metal-organic frameworks (MOFs). Despite of a surge of studies on molecular and ion recognition by MOFs,[2] there are relatively less examples on such recognition by the assemblies of metal complexes.[3] However, an interplay of dative bonds, hydrogen bonds and π-stacking interactions can be applied for the efficient stabilization of supramolecular structures, suggesting a possibility of utilization of derived frameworks for molecular recognition.[4] Anionic[5] or cationic[6] supramolecular assemblies also serve as templates in molecular recognition. Among anionic assemblies, metal dipicolinate complexes[7] are extensively studied; they generally self-assemble through π-stacking interactions as illustrated in Figure 1a and are useful to selectively bind cations. Besides conventional stacking patterns of dipicolinate complexes, there are other ways of π-stacking (Figure 1b) that would also lead to layered structures. We have previously shown that layered structures of dipicolinate complexes of divalent metal ions are guided by cations.[7l] Sevov and co-workers investigated guest-free and guest-included frameworks assembled from the anionic metal complexes of bipyridinium cations.[8] However, molecular recognition in π-stacking assemblies comprising of complex anions have not been addressed in detail. There were also no attempts to segregate layered structures for the generation of discrete units by competitive π-interactions.

It was earlier shown that organic motifs derived from naphthlenediimide,[9a] phthalimide,[9b-c] and pyromellitic diimide[9d] are capable of holding hydroxyaromatic compounds, resulting in host-guest complexes with interesting properties. On the basis of π-stacking interactions it was also possible to distinguish planar polyaromatic hydrocarbons by spectroscopic changes or by visual means. Thus, the design of a pi-stacking template to hold planar aromatic compounds is of great interest, while the control of such template by organic cations to modulate different spaces in

between π-stacks to a guest molecule is of challenge. In an earlier study,[9d] it was shown that methanol solvent changes the self-assembly of N,N′-bis(glycinyl)pyromellitic diimide enabling the binding of guest molecules, which otherwise could not have been accommodated in a motif constructed without a solvent bridge. Holman and Ward[1g] used directional properties and size of anionic organic host for inclusion of cations of nucleobases. However, an idea to modify area around a template to accommodate guest molecule has not been adopted with anionic templates capable of forming layered complexes by π-stacks. Thus, we have followed such a modular approach to change the π-stacking pattern of dipicolinate complexes, which are known to π-stack and can control π-stacking patterns by variation of cations.

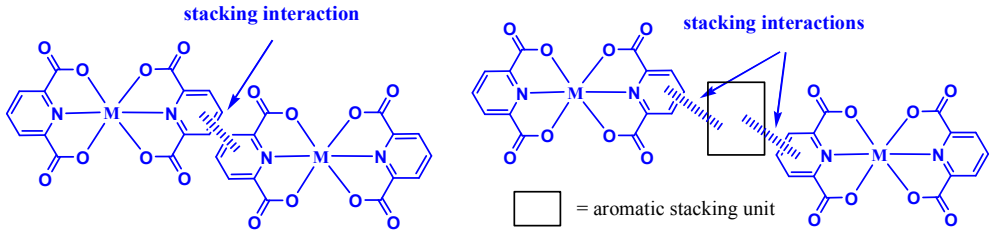

(a) (b)

Figure 1: Two different ways of π-stacking arrangements to form layered structures in metal dipicolinate complexes.

To reason out which packing pattern would be useful in molecular recognition, we have prepared two parent zinc dipicolinate complexes with the geometrically distinct 4,4'-bipydinium or 1,3-bis(4-pyridinium)propane cations, $[H_2tmbpy][Zn(pdc)_2]\cdot 5H_2O$ (**1**) and $[H_2bpy][Zn(pdc)_2]\cdot 6H_2O$ (**2**). Given that these compounds have a wide difference in flexibility for molecular recognition study, we have investigated the reactions of **1** and **2** with various phenolic compounds listed in Scheme 1. As a result, a series of host-guest derivatives **3**–**7** has been generated (Scheme 2) and fully characterized by IR and ^{1}H-NMR spectroscopy, thermogravimetric analyses. Crystal packing patterns and topological features of complexes **1-2** and **5-7** have been analyzed. Besides, the molecular recognition of 4-nitrophenol by **2** to form an adduct **3** has been studied by UV-vis and ^{1}H-NMR spectroscopic methods.

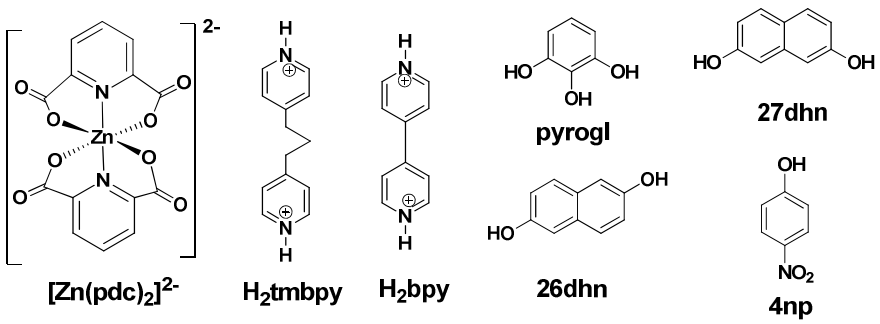

Scheme 1: Zinc dipicolinate anion, organic cations and guest molecules.

Results and Discussion

Synthesis of 1–7. As illustrated in Scheme 2, the parent zinc dipicolinate complexes $[H_2tmbpy][Zn(pdc)_2]\cdot 5H_2O$ (**1**) and $[H_2bpy][Zn(pdc)_2]\cdot 6H_2O$ (**2**) were self-assembled from aqueous solutions of $Zn(OAc)_2\cdot 2H_2O$, dipicolinic acid and 1,3-bis(4-pyridyl)propane or 4,4′-bipyridine. These complexes were then treated with various phenolic compounds resulting in crystallization of a series of adducts with 4-nitrophenol (**3**), 2,7-dihydroxynaphthalene (**4**, **5**), pyrogallol (**6**), and 2,6-dihydroxynaphthalene (**7**). All the products were isolated as crystalline solids in good yields and were characterized. In an earlier study,[10] the reaction of zinc sulphate with 2,6-pyridinedicarboxylic acid in hot water resulted in two types of crystals, $[Zn(H_2O)_5Zn(pdc)_2]\cdot 2H_2O$ and $[Zn(Hpdc)_2]\cdot 3H_2O$. In the present work, we carried out reactions at room temperature in H_2O at pH ~5 using $Zn(OAc)_2\cdot 2H_2O$ and H_2pdc (1:2 molar ratio), and obtained only a mononuclear product $[Zn(Hpdc)_2]\cdot 3H_2O$. Its composition was confirmed by comparison with an authentic sample.[10] Further, we added amines to these reactions to form counterions, which generally help in the stabilization of mononuclear zinc dipicolinate complexes.[6l] These inclusion reactions pass through $[Zn(Hpdc)_2]\cdot 3H_2O$, while the formation of a dinuclear zinc complex in the absence of an amine cation is one of the reasons leading to inclusion complexes.

The number of crystallization water molecules present in each case can be substantiated by thermogravimetry. All the complexes exhibit a weight loss below 200 °C due to removal of water molecules (Figure S4-10S); such weight loss shows a very close correlation with the amount of water present in each compound. Thermogravimetry analyses of **1**–**5** reveal that they decompose to produce zinc oxide on heating in the 380-420 °C range.

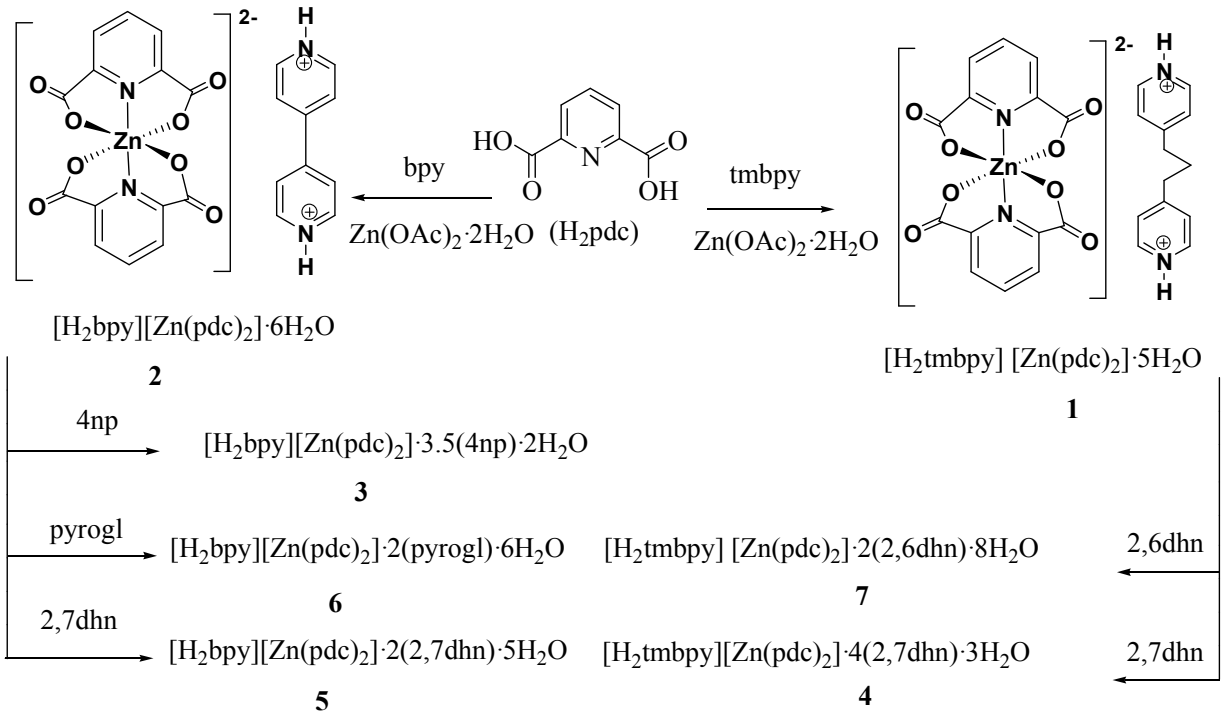

4np = 4-nitrophenol, pyrogl = pyrogallol, 2,7dhn = 2,7-dihydroxynaphthalene,
2,6dhn = 2,6-dihydroxynaphthalene; bpy = 4,4'-bipyridine, tmbpy = 1,3-bis (4-pyridine)propane

Scheme 2: Synthesis of parent compounds **1** and **2** and their various guest included derivatives **3**–**7**.

Structures of 1 and 2. Complexes **1** and **2** possess the same anionic unit, $[Zn(pdc)_2]^{2-}$ but different cations. Drastic differences in packing patterns of these two complexes are observed. Compound **1** has a layered structure that is similar to the earlier reported structures of dipicolinate derivatives constituted by layers of anionic complexes formed through π-interactions as illustrated in Figure 1a. In this case, there is a distance of ~3.5 Å between the pyridine rings of parallel dipicolinate moieties from two independent anions. This distance is reasonable for π-interactions (Figure 2a). On the other hand, other dipicolinate ligand present in the same molecule also stacks parallel with a similar counterpart of neighboring molecule, but they are not involved in π-interactions; instead, they are connected to corresponding counterpart of the adjacent molecule through C4-H···O6 interactions. On the other hand, complex **2** (Figure 2b) has a large π-separation (~4.2 Å) between the pyridine rings of $[Zn(pdc)_2]^{2-}$ which, however, adopt suitable geometry to participate in π-interactions with 4,4′-bipyridinium cations. Thus,

packing is guided by the host-guest-host types of π-stacking arrangements. It is known that highly π-stacking cations (e.g., quinolinium cations) tend to disrupt the π-stacking of anions and inhibit the formation of conventional layered structures of dipicolinate complex anions.[7l] On the other hand, the presence of planar π-ligands such as 1,10-phenanthroline or 2,2′-bipyridine provides multiple ways of π-stacking arrangements in a dipicolinate complex.[1g] Since bis-dipicolinate complexes have two π-aromatic rings around metal ion, they may be compared with other compounds bearing π-stacking ligands such as 1,10-phenanthroline. In this regard, penta-coordinate copper(II) sulphate complexes with two 1,10-phenanthroline ligands have an overlapping of both π-aromatic units to form chains, but the extent of the π-stacking overlap zone is decided by the fifth donor atom (ligand) as well as solvent of crystallization.[11] Thus, in our case the observation on the differences in π-stacking by $[H_2bpy]^{2+}$ and $[H_2tmbpy]^{2+}$ ions is attributed to packing requirements, which are finally guiding the directional interactions.

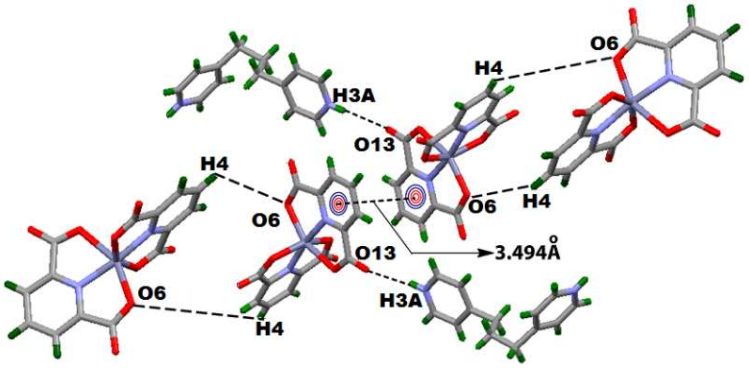

(a)

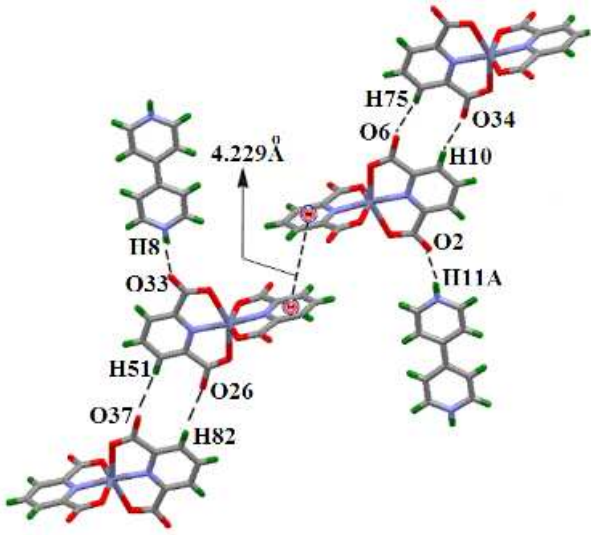

(b)

Figure 2: Structural fragments of complexes (a) **1** and (b) **2** showing some important interactions.

Molecular recognition of 4-nitrophenol.

Molecular recognition of hydroxy-substituted aromatic guests by hydrogen bonds and π-π interactions is common.[12] Planar nature of aromatic hydrogen-bond receptor molecules improves significantly the complexation ability of a guest by assisting in π-stacking interactions.[13] Some host molecules can accommodate neutral aromatic guests between two aromatic surfaces.[14] Hydroxyaromatic compounds can also act as guests of crown ethers.[15] In the present work, we found an interesting example of selective binding of 4-nitrophenol with complex **2** to give an adduct **3** (Scheme 2). We observed that the addition of an aqueous solution of 4-nitrophenol to an aqueous solution of complex **2** leads to a steady growth of an absorption peak at 432 nm in the UV-vis spectrum (Figure 3a). This band occurs at a wavelength 36 nm higher than the absorption peak of 4-nitrophenol (396 nm). On the other hand, there is no interaction between 4-nitrophenol in a similar experiment with complex **1**, as no shift in absorption on titration with **1** was detected and in this case there was an increase in absorption at 396 nm as concentration of 4-nitrophenol increased in solution during titration. Complex **3** has the ^{1}H-NMR signals at 6.73 and 7.92 ppm from $[H_2bpy]^{2+}$, 7.40 and 8.56 ppm due to 4-nitrophenol, and at 8.21 and 7.70 ppm from dipicolinate. Correlation observed between the signals a and d, b and f, c and e, in the ^{1}H-HOMOCOSY spectra (Figure 3ii) confirms the identity of these signals. Since 4-nitrophenol can be considered as a weak acid and 4,4′-bipyridine is a weak base, both can interact to form an adduct. This was experimentally confirmed while comparing the independent ^{1}H-NMR spectra of 4-nitrophenol and 4,4′-bipyridine with that of an equimolar mixture containing both of them (Figure 3iii). Thus, most likely complex **2** interacts with 4-nitrophenol to form $[Zn(Hpdc)_2]$ and the adduct of 4-nitrophenol with 4,4′-bipyridine. However, the chemical shifts of the guest included complex differ from those of an equimolar mixture of 4np and bpy. This indicates that **2** is responsible for the generation of an inclusion complex with 4-nitrophenol.

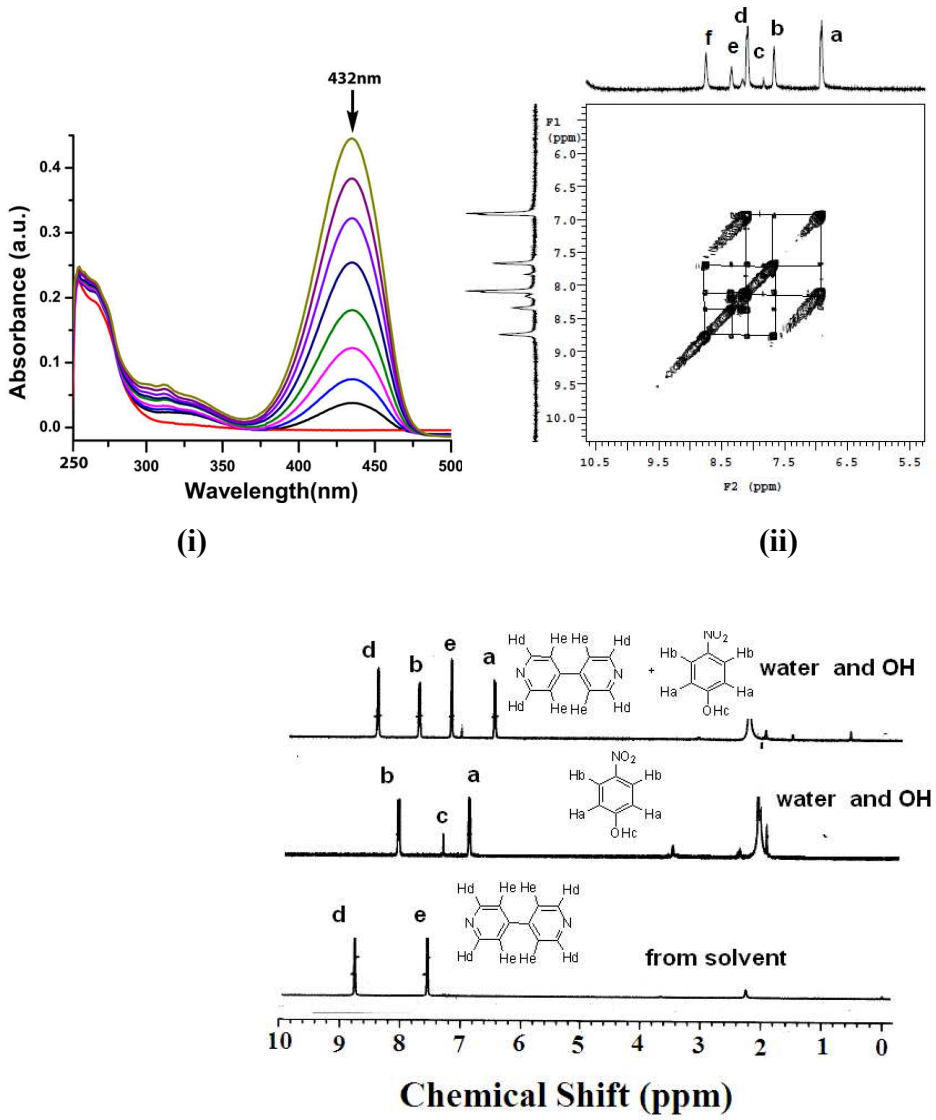

Figure 3: (i) Evolution of UV-vis spectra on addition of 4-nitrophenol (10^{-3} M in water, 50 µL in each aliquot) to an aqeous solution of complex **2** (2 mL of 10^{-3} M in water, 50 µL in each aliquot) showing an increase in absorbance at 432 nm. (ii) ^{1}H-HOMOCOSY spectra (400 MHz, DMSO-d_6; 5.5-10 ppm region) of complex **3**. (iii) ^{1}H-NMR spectra (DMSO-d_6) of 4,4′-bipyridine, 4-nitrophenol, and a mixture of bpy and 4np.

Compound **2** recognizes 4-nitrophenol to give adduct **3**, whereas the parent complex **1** does not form any adduct with 4-nitrophenol. In fact, crystallization of a solution of **1** and 4-nitrophenol yielded the respective parent compounds. We did not get a good single crystal structure of **3** due

to disorder which was not fully resolved due to poor data quality but the skeleton observed from data shows that it has 4-nitrophenol molecules placed in between π-stacks of anions. Thus, the $[H_2bpy]^{2+}$ cation plays a role in the selective recognition of 4-nitrophenol by **2**. Recognition of 4-nitrophenol is attributed to the difference in layer formed by the anions in **1** which does not permit intercalation, but in packing of **2** the cationic part contributes to stacking, which can be replaced by the 4-nitrophenol. This is reflected in the visible spectra during titration of complex **2** with 4-nitrophenol (Figure 3i). 4-nitrophenol and several dihydroxy-aromatic compounds could be recognized on the basis their different binding abilities to organogels.[14f] 4-Nitrophenol is a high impact pollutant, which can be recognized by siloxane based molecularly imprinted polymers[14g] and some nano-particles containing polymers.[14h] Metal-organic frameworks[14i] can also selectively reduce 4-nitrophenol. In comparison to the above-mentioned systems, complex **2** can be easily prepared from commonly available and low-cost commercial reagents and isolated as a single solid product with or without 4-nitrophenol guest, thus generating definite interest to explore similar metal dipicolinate compounds for molecular recognition of various organic molecules.

Formation 4-5 and structure of 5. It was also observed that complexes **1** and **2** independently interact with 2,7-dihydroxynaphthalene to form complexes $[H_2tmbpy][Zn(pdc)_2]\cdot 4(2,7dhn)\cdot 3H_2O$ (**4**) and $[H_2bpy][Zn(pdc)_2]\cdot 2(2,7dhn)\cdot 5H_2O$ (**5**), respectively. For example, ^{1}H-NMR spectrum of an equimolar mixture of 4,4'-bipyridine and 2,7-dihydroxynaphthalene shows that the chemical shifts of the bpy and 2,7dhn protons were changed. Complexation induced ^{1}H-NMR shifts were previously observed on interactions of different phenolic guest molecules (e.g., 2,7-dihydroxynapthalene) with diphenylglycoluril.[16]

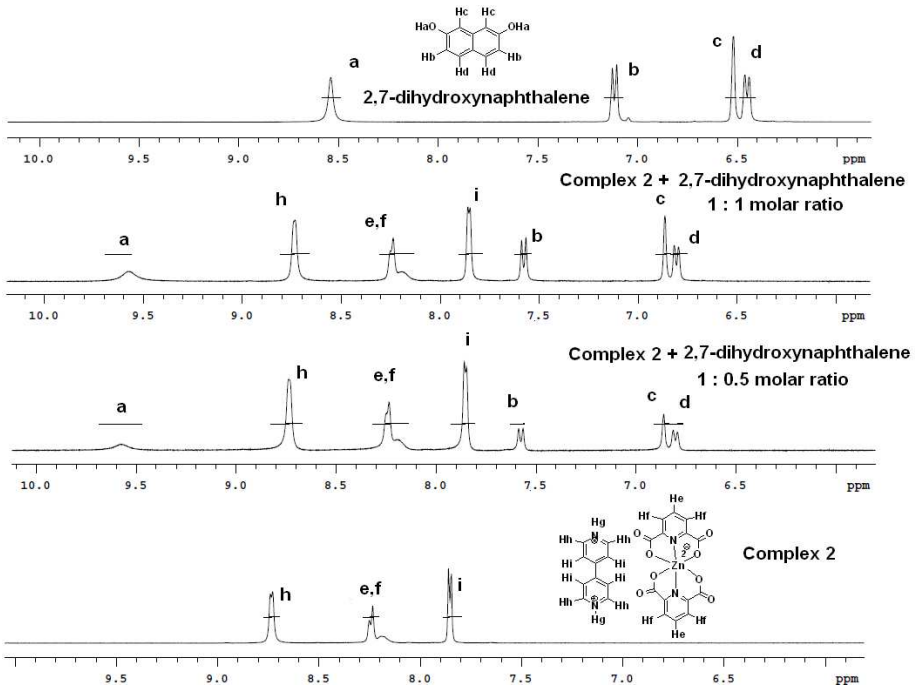

Figure 4: ^{1}H-NMR (DMSO-d_6) spectra of complex **2**, 2,7-dihydroxynaphthalene and **2** with different amounts of 2,7dhn.

In the present case, we have recorded the ^{1}H-NMR spectra of **2** in DMSO-d_6 before and after addition of 2,7-dihydroxynapthalene in 1:0.5 and 1:1 molar ratio. Comparison of the obtained spectra showed that the signals of 2,7dhn were shifted up-field due to interaction with complex **2**. The OH signals of the 2,7-dihydroxynaphthalene are influenced to a greater extent as they broaden and appear at 9.6 ppm. Signals of the H_2bpy and dipicolinate moieties are shifted from downfield with respect to the original peaks of **2** (Figure 4), suggesting interactions between these components in the complex. It may be noted that due to acid-base properties of the 2,7dhn and bpy they interact with each other, and the chemical shifts of a mixture of 2,7-dihydroxynaphthalene and 4,4'-bipyridine in DMSO-d_6 differ from the individual counterpart as illustrated in Fig. 5S. These observations suggest that **2** is responsible for the formation of the inclusion complex. A similar comparison of ^{1}H-NMR signals of complex **4** with 2,7dhn and tmbpy and the equimolar mixture of the latter two components, shows the acid-base interactions between 2,7dhn and tmpby (Figure 1S). On the other hand, ^{1}H-NMR signals of 2,7dhn and tmbpy in **4** are also different in terms of chemical shifts from such adducts of 2,7dhn and tmpby.

Hence, in this case compound **1** can probably act as the template to form an inclusion complex with 2,7dhn, resulting in the generation **4**. The spectral patterns observed in the parent zinc dipicolinate complexes in solution support the formation of an inclusion compound by the π-stacking of the aromatic units, as well as via the interactions of the cations with 2,7dhn; in fact, π-stacking in metal complexes[17a] and hydrogen bond interactions[17b] in phenol-pyridine systems are established. Stoddart and co-workers[18] have demonstrated the utility of bipyridinium functionalized cyclophane scaffolds as π-deficient blocks for the preparation of innumerable interlocked supramolecules, but the host-guest formation ability of bipyridine or bipyridinium cations with 2,7-dihydroxynaphthalene are not strong enough to form isolable host-guest complexes.[31]

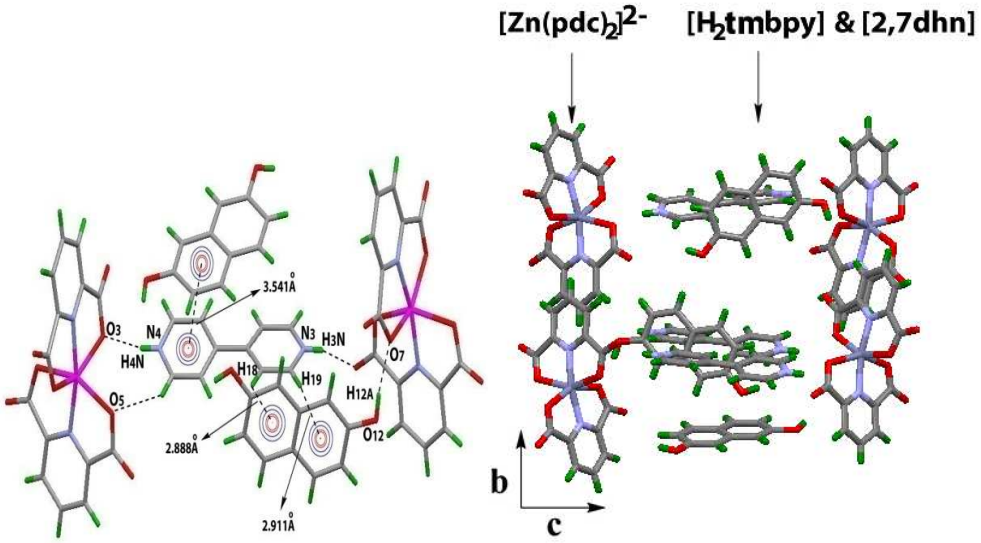

Figure 5: (a) Various interactions between cations, anions, and guest molecules in crystal structures of complex **5**. (b) Packing diagram showing zinc dipicolinate layer motifs in the structures of complex **5**.

Cocrystal **5** possess conventional layered arrangement (Figure 5a). Dihydroxynaphthalenes and cations have stacking interactions among themselves, remaining in between the layers formed by anions. This occurs due to strong contacts between [H_2tmbpy] or H_2bpy with 2,7dhn, which force an anionic part to adopt conventional л-stacking to accomodate cations together with guest molecules. In the case of **5**, we observe reorganisation of original π-stacked arrangement present in **2** while accomodating guest molecules. In **5**, bipyridinium cations interact with two adjacent layers of anions through $–NH^{+}\cdots{}^{-}OOC–$interactions. Guest 2,7dhn molecules also participate in

hydrogen bonds with anions and there is a π-stacking between 2,7dhn and organic cations (Figure 5b).

Formation and structures of 6 and 7. Pyrogallol also forms an adduct $[H_2bpy][Zn(pdc)_2]\cdot 2(pyrogl)\cdot 6H_2O$ (**6**) on treatment with the parent complex **2**. In contrast, recrystallization of **1** with pyrogallol does not result in the generation of adduct. However, 2,6-dihydroxynaphthalene forms an adduct $[H_2tmbpy][Zn(pdc)_2]\cdot 2(2,6dhn)\cdot 8H_2O$ (**7**) with **1** but no such product was obtained when using **2**. Both adducts **6** and **7** have conventional stacking patterns of anions forming layers to hold cations and guest molecules. Charge-assisted hydrogen bonds and π-stacking are dominant interactions that stabilize their packing patterns (Figure 6a and 6b). From these results it is clear that the layered structures by stacking of zinc dipicolinate anions are favored to hold various phenolic compounds, and the process of guest inclusion and adduct formation is largely influenced by the selection of $[H_2bpy]^{2+}$ or $[H_2tmbpy]^{2+}$ cations in host molecules.

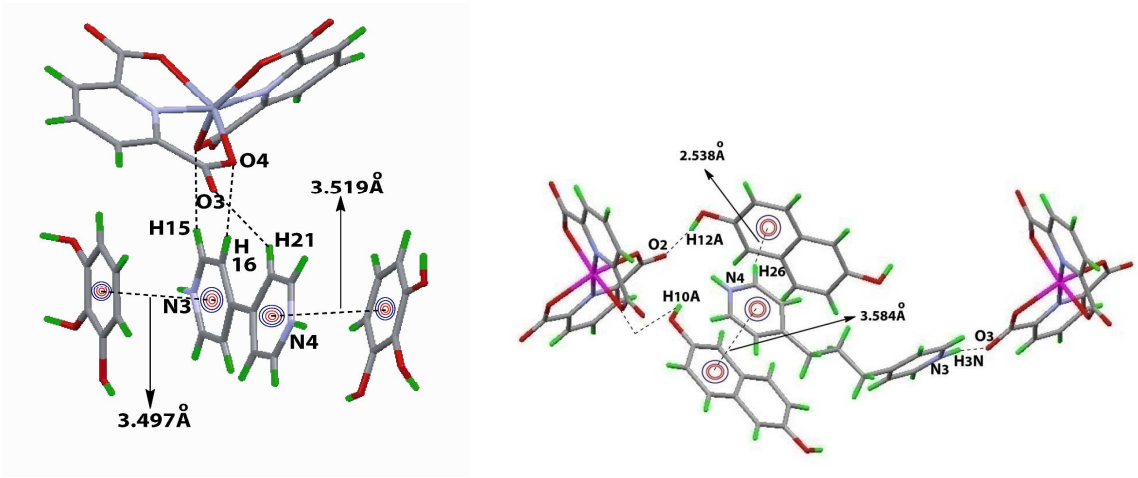

Figure 6: Structural fragments of complexes (a) **6** and (b) **7** showing π-stacking and other interactions.

^{1}H-NMR spectra of complexes **6** and **7** in DMSO-d_6 showed typical signals for the respective cations, dipicolinate anions, and guest molecules. Comparison of the ^{1}H-NMR signals in complexes with the "free" guests indicates that their chemical shifts differ. Pyrogallol shows two

multiplets in aromatic region due to two magnetically non-equivalent protons in 1:2 ratio; these two peaks are shielded in the inclusion complex **6** as illustrated in Fig. 3S. Dipicolinate ligands in the complex exhibit the signals at 8.3 and 8.05 ppm due to pyridine protons. In addition, there are signals at 6.65 and 7.45 ppm corresponding to two sets of aromatic protons of bipyridinium cation. Similarly, complex **7** also carries signature of each component but with different chemical shifts in comparison with those of the constituent molecules. The ^{1}H-NMR signals are compared in an overlaid diagram (see Fig. 4S) with assignment of individual peaks. In these two complexes, we have also observed that despite of acid-base interaction between the phenolic component and the corresponding amine, the amine remains as a cationic counterpart of the complex, thus facilitating the formation of a host-guest compound. Hence, the ^{1}H-NMR study revealed the following important aspect. Although there is a possible synergic effect of the bipyridine molecules to bring the host to form self-assembly and to get included in neutral complex [Zn(Hpdc)$_2$], this is not the case in solution since chemical shifts of the phenolic guest included complexes are different if compared with those of the equimolar mixture of the corresponding organic compounds.

Topological analysis of H-bonded motifs in 1–2 and 5–7. Apart from various π-stacking interactions, the structures of the determined structures of the complexes reveal a number of strong hydrogen bonds. To understand the crystal packing patterns driven by these hydrogen bonds between the $[Zn(pdc)_2]^{2-}$ anions, $[H_2bpy]^{2+}$ or $[H_2tmbpy]^{2+}$ cations and guest molecules (27dhn, pyrogl, and 26dhn), we have applied a topological analysis method.[19] Following the concept of simplified underlying net, all metal-organic and organic moieties in these structures were reduced to their centroids, giving rise to underlying H-bonded motifs. These motifs were generated by considering only the conventional (strong) hydrogen bonds D–H···A [H···A <2.50 Å, D···A <3.50 Å, ∠(D–H···A) >120°; D and A stand for donor and acceptor atoms].[19a] The obtained motifs were topologically classified[13] and the results are represented in Figure 7.

In the parent compound **2**, the $[Zn(pdc)_2]^{2-}$ anions and $[H_2bpy]^{2+}$ cations form simple 0D dimeric motifs with the 1M2-1 topology (Figure 7a). These 1D chains are packed into 2D layered motifs that are also mutually interdigitated. Such a dense interdigitation and multiple H-bonding of 4-nitrophenol can also explain the observed recognition of this guest by the zinc dipicolinate host. Compound **2** transforms to **5** upon recrystallization with 2,7-dihydroxynaphthalene, wherein the

1D zigzag H-bonded chain motifs can be identified (Figure 7b). These are assembled from the 2-connected $[Zn(pdc)_2]^{2-}$ and $[H_2tmbpy]^{2+}$ nodes and the 1-connected dangling 2,7dhn moieties, leading to the 2C1 topology. The zigzag chains in **5** are not interdigitated. In **6**, the use of pyrogallol as a guest leads to a 2D H-bonded motif (Figure 7c) that can be topologically classified as the 3-connected layer with the hcb [Shubnikov hexagonal plane net/(6,3)] topology defined by the point symbol of (6^3). This layer is built from the 3-connected topologically equivalent $[Zn(pdc)_2]^{2-}$ and pyrogl nodes, as well as the 2-connected $[H_2bpy]^{2+}$ and pyrogl linkers.

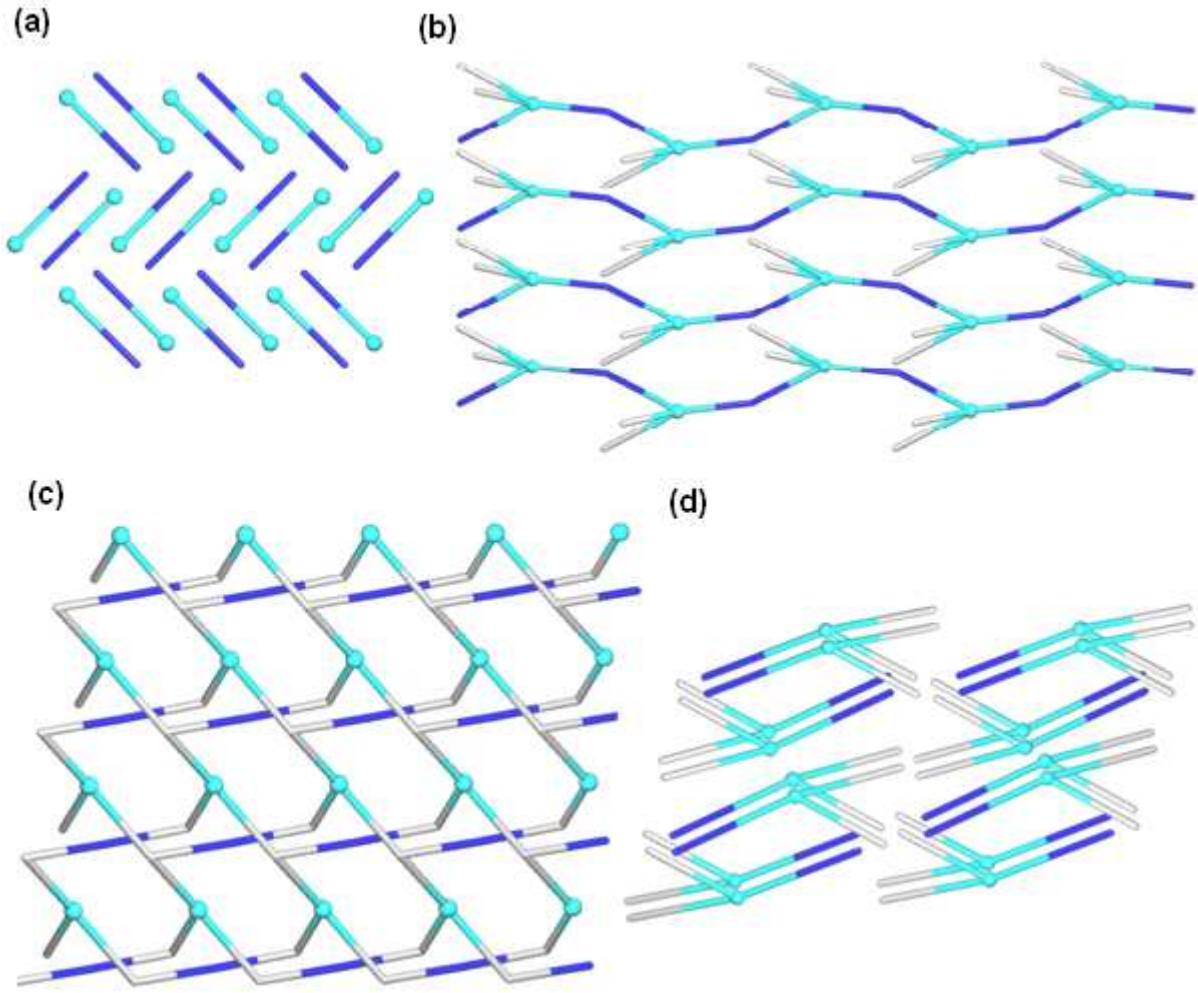

Figure 7: Topological fragments of the simplified H-bonded motifs between $[Zn(pdc)_2]^{2-}$ and organic moieties in **2** (a), **5** (b), **6** (c) and **7** (d). Further details: (a) 1-connected 0D dimeric motifs with the 1M2-1 topology (topologically similar motifs are also observed in **1**); (b) 2-connected 1D chain motifs with the 2C1 topology; (c) 3-connected 2D layer with the hcb topology and point symbol of (6^3); (d) 1,3-connected 0D tetrameric motifs with the 1,3M4-1 topology. Views along the *a* (a), *b* (d) or *c* (b,c) axis. Color codes: centroids of $[Zn(pdc)_2]^{2-}$ blocks (cyan balls),

centroids of $[H_2bpy]^{2+}$ and $[H_2tmbpy]^{2+}$ moieties (blue), centroids of pyrogl, 27dhn and 26dhn guests (gray).

Similarly to **2**, an H-bonding interaction between the $[Zn(pdc)_2]^{2-}$and $[H_2tmbpy]^{2+}$ ions in the parent complex **1** also results in the formation of simple 0D dimeric motifs with the 1M2-1 topology. Its topological classification revealed the 5-connected double 2D layer with the SP 2-periodic net (4,4)Ia topology and point symbol of $(4^8.6^2)$. This intricate double layer is assembled from the 5-connected $[Zn(pdc)_2]^{2-}$ nodes and 2-connected $[H_2bpy]^{2+}$ and 27dhn linkers. In contrast, the 2,6-dihydroxynaphthalene adduct **7** reveals simpler 1,3-connected 0D tetrameric motifs with the 1,3M4-1 topology (Figure 7d).

In summary, these topological findings confirm that the type of H-bonded pattern depends on the selection of $[H_2bpy]^{2+}$ or $[H_2tmbpy]^{2+}$ cations and guest molecules. The parent complex **2** tends to result in infinite H-bonded motifs (i.e., different 1D chains in **5** or 2D layers in **6**), whereas both finite 0D (in **7**) motifs were identified in the complexes derived from **1**.

Water clusters in the crystal structures. In majority of the obtained Zn dipicolinate derivatives, the crystallization water molecules are assembled into different discrete water clusters (Figure 8), ranging from dimers and trimers in **7** to tetramers in **1** and distinct pentamers in **2**, **5** and **6**. All these water associates can be classified within the *D*2 (Figure 8a), *D*3 (Figure 8b), *D*4 (Figure 8c,d) and *D*5 (Figure 8e) type according to the systematization introduced by Infantes and Motherwell.[20] These data confirm[21] that metal dipicolinate complexes are suitable matrices to host various water clusters. Such water associates and discrete water molecules (optional) are also responsible for the extension of the above-discussed H-bonded motifs into 3D (in **1**, **2**, **5**–**7**) supramolecular networks.

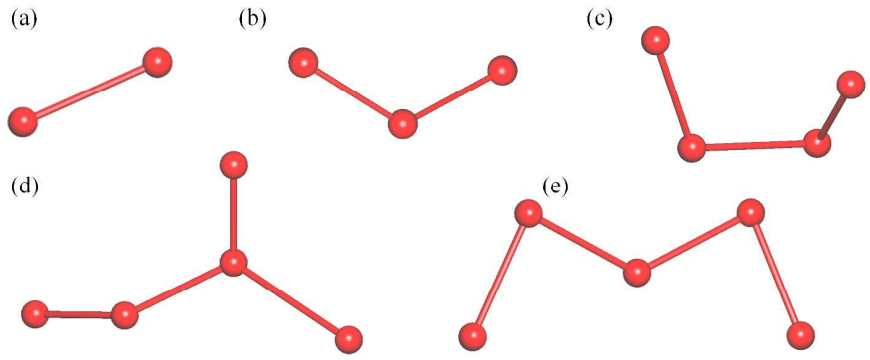

Figure 8: Discrete water clusters identified in the crystal structures: (a) $(H_2O)_2$ dimer in **7**, (b) $(H_2O)_3$ trimer in **7**, (c) $(H_2O)_4$ tetramer in **1**, (d) branched $(H_2O)_5$ pentamer in **2**, (e) $(H_2O)_5$ pentamer in **6.**

Since we have observed different types of interactions to hold water molecules in the groves of the anions and cations, only the principal hydrogen bonds holding the water clusters are listed in Table 1.

Table 1: Donor-acceptor interactions in water clusters[#]

Complex	Type of water cluster	Type of interactions (number of interactions)
1	$(H_2O)_4$	$C{=}O_{dipic}\cdots H$ (four); $O_{dipic}\cdots H\text{-}O_{water}$ (one); $N^{+}\text{-}H\cdots O_{water}$ (one)
2	$(H_2O)_5$, branched	$C{=}O_{dipic}\cdots H\text{-}O_{water}$ (one); $O_{dipic}\cdots H\text{-}O_{water}$ (two); $N^{+}\text{-}H\cdots O_{water}$ (one)
5	$(H_2O)_5$	$O_{nap}\cdots H\text{-}O_{water}$ (three); $O_{dipic}\cdots H\text{-}O_{water}$ (two); $C{=}O_{dipic}\cdots H$ (one); bifurcated $C{=}O_{dipic}\ldots H$ (one);
6	$(H_2O)_5$	$O_{pyr}\cdots H\text{-}O_{water}$ (three); $C{=}O_{dipic}\cdots H$ (three); $O_{dipic}\cdots H\text{-}O_{water}$ (two)
7	$(H_2O)_2$ $(H_2O)_3$	$O\text{-}H\cdots O_{water}$ (two); $C{=}O_{dipic}\cdots H\text{-}O_{water}$ (one). $O_{dipic}\cdots H\text{-}O_{water}$ (two); $C{=}O_{dipic}\cdots H\text{-}O_{water}$ (two).
#Subscript shown in type of interaction refers to the donor or acceptor atom attached to a unit namely, dipic = dipicolinate; nap = naphthalenenediol, pyr = pyrogallol.		

Tetrameric water cluster of complex **1** is in a grove of four dipicolinate anions and a cation, and is held by one $N^{+}\text{-}H\cdots O$ interaction with $[H_2tmbpy]^{2+}$ and three $C{=}O\cdots H\text{-}O_{water}$ and one $O\cdots H\text{-}O_{water}$ interactions with dipicolinate units. Thus, the outer periphery is guided by water molecules acting as donors at four sites and acceptors at one site. It is also seen that the pentameric water clusters are formed in different ways and the hydroxyl groups on the aromatic rings and the carboxylate groups of dipicolinates have dictated the structure of such clusters. In case of **7**, cluster of two water molecules at one end has a $C{=}O_{dipic}\cdots H\text{-}O_{water}$ interaction and at other end shows two $O\text{-}H\cdots O_{water}$ interactions, thus revealing that the presence of same cations and anions

but two different isomers of dihydroxynaphthalene makes the difference in the donor-acceptor binding schemes of the water dimers.

Conclusions

In the present study, we have prepared and fully characterized a new series of zinc dipicolinate compounds that show two distinct types of π-stacking arrangements. Based on the ability to replace cationic species stacked between dipicolinate groups a modular approach to recognize 4-nitrophenol has been achieved and investigated in detail. We have also established that the supramolecular interactions between the host cations in an anionic metal complex with different hydroxyaromatic guest molecules can set apart the cationic and host fragments from the anionic part, thus allowing an accommodation of both cations and guests in between layered zinc dipicolinate anionic motifs.

Besides, the topological classification of H-bonded patterns driven by strong hydrogen bonds between the $[H_2bpy]^{2+}$ or $[H_2tmbpy]^{2+}$ cations and $[Zn(pdc)_2]^{2-}$ anions, and organic guest molecules has been performed, disclosing the finite 0D (in **1**, **2**, and **7**) and infinite 1D (in **5**) or 2D (in **6**) topological motifs. Although H-bonded chains in **5** are topologically similar. The topological findings attest that the type of H-bonded pattern is significantly influenced by the selection of bipyridinium cations and guest molecules.

Experimental:

General.

IR spectra were recorded on a PerkinElmer Spectrum One FTIR spectrophotometer with KBr disks in the range 4000−400 cm^{-1}. Thermogravimetric analysis was performed using a Mettler Toledo instruments simultaneous DTA/TGA system, under nitrogen with a heating rate of 7 °C/min. Electronic spectra were recorded using Perkin-Elmer Lamda-750 spectrometer. ^{1}H-NMR spectra were run on Bruker 400MHz spectrometer. ^{1}H-NMR spectra were recorded by dissolving the samples in DMSO-d_6. The ^{1}H-NMR titration of complex **2** with 2,7-dihydroxynapthalene was carried out by recording two independent spectra at 18 °C, using the solutions of **2** with 2,7-dihydroxynapthalene in 1:0.5 and 1:1 molar ratio. UV-visible titration was done by taking a 2 ml solution (10^{-3} M) of complex **2** dissolved in deionised water in a

quartz cuvette and absorption spectra was recorded, to this aqueous solution of 4-nitrophenol was added in aliquots of 50 μL and after each addition UV-visible spectra was recorded.

Synthesis and characterization of 1-7. $[H_2tmbpy][Zn(pdc)_2]\cdot 5H_2O$ (1) and $[H_2bpy][Zn(pdc)_2]\cdot 6H_2O$ (2). To an aqueous solution (20 mL) of dipicolinic acid (0.167 g, 1 mmol), an aqueous solution of $Zn(O_2CCH_3)\cdot 2H_2O$ (0.109 g, 0.5 mmol) was added and stirred for half an hour. A white precipitate was obtained. The pH of the solution was measured and found to be ~5. The solid obtained from this reaction was further reacted with a heterocyclic compound (0.5 mmol in 20 mL methanol), namely 1,3-bis(4-pyridine)propane for **1** or 4,4'-bipyridine for **2**, in independent experiments to obtain a homogeneous solution in each case. The solutions, on standing at room temperature, resulted in the formation of crystals of **1** and **2** after 3-4 days.

(1) Isolated yield 70%. IR (KBr, cm^{-1}): 3443 (br), 3086 (w), 2138 (w), 1629 (s), 1490 (w), 1431 (w), 1375 (s), 1277 (m), 1184 (w), 1076 (w), 980 (w), 909 (w), 818 (m). ^{1}H-NMR (400 MHz, $CDCl_3$): δ (ppm) 8.49 (m, 4H), 8.40 (d, J = 8Hz, 4H), 8.15 (t, *J* = 8 Hz, 2H), 7.12 (m, 4H), 3.50 (broad, D_2O-exchangeable protons), 2.68 (m, 4H), 2.02 (m, 2H).

(2) Isolated yield 72%. IR (KBr, cm^{-1}): 3415 (br), 3074 (w), 2924 (w), 1634 (s), 1502 (m), 1427 (w), 1375 (s), 1276 (m), 1189 (m), 1078 (m), 1034 (m), 913 (m), 793 (m), 677 (m). ^{1}H-NMR (400 MHz, $CDCl_3$, ppm): 8.75 (d, *J* = 8 Hz, 4H), 8.39 (d, *J* = 8 Hz, 4H), 8.15 (t, *J* = 8 Hz, 2H), 7.59 (d, *J* = 6Hz, 4H), 3.50 (broad, D_2O-exchangeable protons).

$[H_2bpy][Zn(pdc)_2]\cdot 3.5(4np)\cdot 2H_2O$ (3). An aqueous solution of **2** (1 mmol, 5 mL) was mixed with an aqueous solution of 4-nitrophenol (0.14g, 1 mmol, 5 mL) and the obtained mixture was left to slowly evaporate in air, giving colorless crystals of **3** in 10 days. Isolated yield: 68%. IR (KBr, cm^{-1}): 3408 (br), 3096 (w), 2957 (w), 2878 (w), 2813 (w), 2743 (w), 2688 (w), 2138 (w), 1633 (s), 1583 (s), 1496 (s), 1435 (w), 1384 (m), 1337 (s), 1286 (s), 1245 (m), 1108 (s), 1075 (m), 1032 (w), 993 (m), 852 (s), 812 (s), 776(w). ^{1}H-NMR (400 MHz, $CDCl_3$, ppm): 8.56 (d, *J* = 8 Hz,4H), 7.92 (d, *J* = 8 Hz, 2H), 7.70 (m, 2H), 7.40 (m, 2H), 6.73 (d, *J* = 8 Hz, 4H), 3.00 (broad, D_2O-exchangeable protons).

$[H_2tmbpy][Zn(pdc)_2]\cdot 4(2,7dhn)\cdot 3H_2O$ (4). An aqueous solution of **1** (1 mmol, 5 mL) was mixed with an aqueous solution of 2,7-dihydroxynapthalene (0.30 g, 2 mmol, 5 mL) and the obtained mixture was left to slowly evaporate in air, leading to the formation of colorless crystals of **4.** Isolated yield: 41%. IR (KBr, cm^{-1}): 3406 (bs), 3086 (w), 2918 (w), 2864 (w), 2714 (w), 2610 (w), 1632 (s), 1500 (w), 1459 (w), 1424 (m), 1281 (m), 1254 (w), 1209 (s), 1151 (m), 1075 (w) 950 (w), 912 (w), 869 (w), 803 (s), 725(w). ^{1}H-NMR (400 MHz, $CDCl_3$, ppm): 8.36 (d, *J* = 8.4 Hz, 4H), 8.26 (d, *J* = 8 Hz, 4H), 8.05 (t, J = 8Hz, 2H), 7.42 (d, *J* = 8.2 Hz,4H), 6.99 (d, *J* = 4.4 Hz, 4H), 6.83 (s, 4H), 6.76 (d, *J* = 6 Hz,4H), 3.0 (broad, broad exchangeable protons), 2.53 (t, *J* = 7 Hz, 4H), 1.86 (m, *J* = 7.2 Hz, 2H).

$[H_2bpy][Zn(pdc)_2]\cdot 2(2,7dhn)\cdot 5H_2O$ (5). An aqueous solution of **2** (1 mmol, 5 mL) was mixed with an aqueous solution of 2,7-dihydroxynapthalene (0.30 g, 2 mmol, 5 mL) and the obtained mixture was left undisturbed to slowly evaporate in air. Reddish, block-shaped crystals of complex **5** were obtained in ten days. Isolated yield 74 %. IR (KBr, cm^{-1}): 3507 (br), 3101 (w), 2965 (w), 2119 (w), 1632 (s), 1512 (m), 1481 (w), 1390 (s), 1312 (m), 1275 (m), 1212 (m), 1153 (w), 1076 (m), 1029 (w), 978 (w), 916 (w), 875 (w), 840 (w), 802 (s), 765 (w). ^{1}H-NMR (400 MHz, $CDCl_3$, ppm): 8.60 (d, J = 8 Hz, 4H), 8.25 (d, J = 8 Hz, 4H), 7.42 (t, J = 8 Hz, 2H), 6.81 (s, 4H), 6.75 (s, 2H), 6.73 (m, 4H), 2.8 (broad, exchangeable protons).

$[H_2bpy][Zn(pdc)_2]\cdot 2(pyrogl)\cdot 6H_2O$ (6). An aqueous solution of **2** (1 mmol, 5 mL) was mixed with an aqueous solution of pyrogallol (0.25 g, 2 mmol, 5 mL) and the obtained mixture was left undisturbed to slowly evaporate in air. Colorless, block-shaped crystals of **6** were obtained in ten days. Isolated yield 68%. IR (KBr, cm^{-1}): 3351 (bs), 2913 (w), 2675 (w), 2150 (w), 1627 (s), 1609 (s), 1466 (m), 1431 (w), 1431 (s), 1391 (s), 1287 (m), 1220 (w), 1184 (w), 1073 (s), 986 (w), 918 (w), 820 (w), 772 (m), 730 (w). ^{1}H-NMR (400 MHz, $CDCl_3$, ppm) 8.65 (m, 4H), 8.30 (d, J = 7.2 Hz, 4H), 8.05 (t, J = 8Hz, 2H), 7.48 (m, 4H), 6.5 (t, J= 7 Hz, 2H), 6.34 (d, J = 8 Hz, 4H), 2.60 (broad, D_2O-exchangeable protons).

$[H_2tmbpy][Zn(pdc)_2]\cdot 2(2,6dhn)\cdot 8H_2O$ (7). An aqueous solution of **1** (1 mmol, 5 mL) was mixed with an aqueous solution of 2,6-dihydroxynapthalene (0.30 g, 2 mmol, 5 mL) and the obtained mixture was left undisturbed to slowly evaporate in air. Reddish, block-shaped crystals of **7** were obtained in ten days. Isolated yield, 69 %. IR (KBr, cm^{-1}): 3407 (bs), 3040 (w), 2612 (w), 2146 (w), 1630 (s), 1593 (s), 1508(w), 1432 (m), 1374 (s), 1280 (w), 1257 (w), 1229 (s), 1147 (w), 1118 (w), 1077 (m), 1038 (w), 937 (w), 913 (w), 859 (s), 797 (w), 772 (m), 729 (m), 681 (w). ^{1}H-NMR (400 MHz, $CDCl_3$, ppm): 8.34 (d, J = 8 Hz, 4H), 8.23 (d, J = 8 Hz, 4H), 7.98 (t, J = 8 Hz, 2H), 7.34 (d, J = 8 Hz, 4H), 6.96 (d, J = 8 Hz, 4H), 6.91 (s, 4H), 6.89 (m, 4H), 2.5 (t, J = 8 Hz, 4H), 1.84 (m, J = 7.6 Hz, 2H).

Single crystal X-ray diffraction. Crystal diffraction data were collected at 296 K with Mo Kα radiation (λ = 0.71073 Å) using a Bruker Nonius SMART CCD diffractometer. SMART software was used for data collection and also for indexing the reflections and determining the unit cell parameters; collected data were integrated using SAINT software.[22] Structures were solved by direct methods and refined by full-matrix least-square calculations using SHELXTL software.[22] All non-hydrogen atoms were refined in anisotropic approximation against F^2 of all reflections. Hydrogen atoms were refined in isotropic approximation and treated as 'riding' in calculated positions. The locations of the H atoms of the protonated organic molecules were justified by difference Fourier synthesis map. In some cases, the H atoms of water molecules were located in the difference Fourier synthesis maps, and refined with isotropic displacement coefficients. Hydrogen atoms of water molecules could not be located in few

occasions. It was also necessary to apply restraints to optimize the distances of some hydrogen atoms of water molecules. Crystal and final refinement parameters are summarized in Table 2.

Table 2: Crystal parameters for complexes **1-2** and **5-7**.

Complex	**1**	**2**	**5**	**6**	**7**
Formula	$C_{27}H_{32}N_4O_{13}Zn$	$C_{24}H_{20}N_4O_{14}Zn$	$C_{44}H_{42}N_4O_{17}Zn$	$C_{36}H_{40}N_4O_{20}Zn$	$C_{47}H_{54}N_4O_{20}Zn$
Formula weight	685.94	653.81	964.19	914.09	1060.31
Crystal system	Triclinic	Monoclinic	Monoclinic	Monoclinic	Monoclinic
Space group	P -1	P 2_1/n	P 2_1/c	P -1	C 2/c
a (Å)	9.4470(2)	15.5716(6)	9.7219(6)	10.6100(7)	35.4376(15)
b (Å)	11.2899(3)	18.7124(7)	31.1721(17)	12.0306(9)	14.2504(6)
c (Å)	14.6544(4)	20.0292(7)	14.6705(8)	15.6789(11)	20.2796(9)
α (deg)	99.037(2)	90.00	90.00	90.00	90.00
β (deg)	101.948(2)	101.267(2)	97.112(3)	98.640(4)	105.902(2)
γ (deg)	94.145(2)	90.00	90.00	90.00	90.00
V (Å^3)	1501.22(7)	5723.7(4)	4411.7(4)	1978.6(2)	9849.3(7)
Z	2	8	4	2	8
$\rho_{calc.}$ (g ·cm^{-3})	1.517	1.517	1.452	1.534	1.430
μ (mm^{-1})	0.891	0.934	0.637	0.710	0.582
F(000)	712	2672	2000	948	4432
Reflns collected	10210	75438	549230	18632	43501
Reflns unique	5157	20345	5613	7225	8610
Ranges (h, k, l)	-11 ≤ h ≤ 9 -13 ≤ k ≤ 12 -6 ≤ l ≤ 17	-16 ≤ h ≤ 22 -22 ≤ k ≤ 22 -24 ≤ l ≤ 23	-11 ≤ h ≤ 11 -35 ≤ k ≤ 36 -15 ≤ l ≤ 17	-12 ≤ h ≤ 12 -14 ≤ k ≤ 14 -14 ≤ l ≤ 18	-42 ≤ h ≤ 42 -15 ≤ k ≤ 15 -25 ≤ l ≤ 23
Completeness to 2θ(deg)	97.4	99.9	99.3	98.3	99.3
GOF (F^2)	0.905	0.991	1.047	1.054	1.071
$R_1[I \geq 2\sigma(I)]$	0.0372	0.0490	0.0495	0.1038	0.0508
wR_2 $[I \geq 2\sigma(I)]$	0.1214	0.1246	0.1674	0.2626	0.1535
R_1 (all data)	0.0448	0.0749	0.0747	0.1108	0.1848
wR_2 (all data)	0.1372	0.1429	0.1825	0.2653	0.1781
Largest diff peak / hole (e Å^{-3})	0.055 / -0.349	0.103/ -0.717	0.067/ -0.290	0.141 / -0.627	0.090 / -0.487

Acknowledgement: Authors thank Ministry of Human Resource and Development, India for Departmental support. AMK acknowledges the FCT (PTDC/QUI-QUI/121526/2010).

Supporting information: Crystallographic information files are deposited to Cambridge Crystallographic Database; CCDC numbers for complex **1** is 1043721, complex **2** is 1043717, complex **5** is 1043716, complex **6** is 1043718 and complex **7** is 1043719. Comparisons of ^{1}H-NMR spectra of **4**, **6** and **7** with their respective ligands, and thermogravimetric traces of **1**–**7** are available.

References:

1. (a) K. T. Holman, A. M. Pivovar, J. A. Swift, M. D. Ward, *Acc. Chem. Res.,* 2001, **34,** 107-118. (b) M. D. Ward, *Chem. Commun.,* 2005, 5838-5842. (c) R. E. Melendez, C. V. K. Sharma, M. J. Zaworotko, C. Bauer, R. D. Rogers, *Angew. Chem. Int. Ed.,* 1996, **35,** 2213-2215. (d) K. Biradha, D. Dennis, V. A. MacKinnon, K. C. V. Sharma, M. J. Zaworotko, *J. Am. Chem. Soc.,* 1998, **120,** 11894-11903. (e) M. W. Hosseini, *Acc. Chem. Res.,* 2005, **38,** 313-323. (f) P. Dechambenoit, S. Ferlay, N. Kyritsakas, M. W. Hosseini, *Chem. Commun.,* 2009, 1559-1561. (g) K. T. Holman, M. D. Ward, *Angew. Chem. Int. Ed.,* 2000, **39,** 1653-1656. (h) B. Das, J. B. Baruah, *J. Mol. Struct.,* 2011, **1001**, 134-138.

2. (a) L. E. Kreno, K. Leong, O. K. Farha, M. Allendorf, R. P. Van Duyne, J. T. Hupp, *Chem. Rev.,* 2012, **112,** 1105-1125. (b) J. Ye, L. Zhao, R. F. Bogale, Y. Gao, X. Wang, X. Qian, S. Guo, J. Zhao, G. Ning, *Chem. Eur. J.,* 2015, **21**, 2029-2037. (c) Y. Gao, X. Zhang, W. Suna, Z. Liu, *Dalton Trans.,* 2015, **44**, 1845-1849. (d) M. Carboni, Z. Lin, C. W. Abney, T. Zhang, W. Lin, *Chem. Eur. J.,* 2014, **20**, 14965-14970.

3. (a) M. W. Hosseini, *Coord. Chem. Rev.,* 2003, **240**, 157-166. (b) H. Tsukube, S. Shinoda, *Chem. Rev.,* 2002, **102,** 2389-2403. (c) V. Blanco, M. Chas, D. Abella, E. Pia, C. Platas-Iglesia, C. Peinador, J. M. Quintela, *Org. Lett.,* 2008, **10,** 409-412. (d) S. Y. Chang, H. Y. Jang, K. S. Jeong, *Chem. Eur. J.,* 2004, **10,** 4358-4366. (e) K. D. Benkstein, J. T. Hupp, C. L. Stern, *Angew. Chem. Int. Ed.,* 2000, **39**, 2891-2893. (f) E. Stulz, S. M. Scott, A. D. Bond, S. J. Teat, J. K. M. Sanders, *Chem. Eur. J.,* 2003, **9**, 6039-6048. (g) D. Xu, B. Hong, *Angew. Chem. Int. Ed.,* 2000, **39**, 1826-1829. (h) A.V. Davis, K. N. Raymond, *J. Am. Chem. Soc.,* 2005, **125,** 7912-7919. (i) M. Yoshizawa, J. Nakagawa, K. Kurnazawa, M. Nagao, M. Kawano, T. Ozeki, M. Fujita, *Angew. Chem. Int. Ed.,* 2005, **44,** 1810-1813. (j) K. Ono, M. Yoshizawa, T. Kato, K. Watanabe, M. Fujita, *Angew. Chem. Int. Ed.,* 2007, **46,** 1803-1806. (k) A. Y. Ziganshina, Y. H. Ko, W. S. Jeon, K. Kim, *Chem. Commun.,* 2004, 806-807. (l) M. D. Garcia, C. Alvarino, E. M. Lopez-Vidal, T. Rama, C. Peinador, J. M. Quintela, *Inorg. Chim. Acta* 2014, 417, 27-37.

4. H.W. Roesky, M. Andruh, *Coord. Chem. Rev.* 2003, **236**, 91-119.

5. (a) J. W. Cai, *Cryst. Growth Des.,* 2012, **12**, 2684-2690. (b) X. Y. Wang, S. C. Sevov, *Chem. Mater.,* 2007, **19**, 4906-4912. (c) X. Y. Wang, S. C. Sevov, *Cryst. Growth Des.,* 2008, **8**, 1265-1270. (d) A. P. Cote, G. K. H. Shimizu, *Chem. Eur. J.,* 2003, **9,** 5361-5370. (e) X. Y. Wang, R. Justice, S. C. Sevov, *Inorg. Chem.,* 2007, **46,** 4626-4631. (f) S. A. Dalrymple, G. K. H. Shimizu, *J. Am. Chem. Soc.,* 2007, **129,** 12114-12116. (g) S. A. Dalrymple, G. K. H. Shimizu, *Chem.*

Commun., 2006, 956-958. (h) S. A. Dalrymple, M. Parvez, G. K. H. Shimizu, *Chem. Commun.,* 2001, 2672-2673. (i) S. A. Dalrymple, M. Parvez, G. K. H. Shimizu, *Inorg. Chem.,* 2002, **41,** 6986-6996. (j) J. W. Cai, X. P. Hu, J. H. Yao, L. N. Ji, *Inorg. Chem. Commun.,* 2001, **4,** 478-482.

6. (a) J. P. Garcia-Teran, O. Castillo, U. Garcia-Couceiro, G. Beobide, P. Roman, *Inorg. Chem.,* 2007, **46,** 3593-602. (b) T. Paris, J. -P. Vinneron, J. -M. Lehn, M. Cesario, J. Guilhem, C. Pascard, *J. Inclusion Phenomena and Macrocyclic Chem.,* 1999, **33,** 191-202. (c) B. Das, J. B. Baruah *Polyhedron,* 2012, **31,** 361-367. (d) C. Garcia-Simon, M. Garcia-Borras, L. Gomez, I. Garcia-Bosch, S. Osuna, M. Swart, J. M. Luis, C. Rovira, M. Almeida, I. Imaz, D. Maspoch, M. Costas, X. Ribas, *Chem. Eur. J.,* 2013, **19**, 1445-1456.

7. (a) J. C. MacDonald, P. C. Dorrestein, M. M. Pilley, M. M. Foote, J. L. Lundburg, R. W. Henning, A. J. Schutlz, J. L. Manson, *J. Am. Chem. Soc.,* 2000, **122**, 11692-11702. (b) A. M. Beatty, K. E. Granger, A. E. Simpson, *Chem. Eur. J.,* 2002, **8**, 3254-3259. (c) A. M. Beatty, C. M. Schneider, A. E. Simpson, J. L. Zaher, *CrystEngComm,* 2002, **4**, 282-287. (d) J. C. MacDonald, M. Luo, G. T. R. Palmore, *Cryst. Growth Des.,* 2004, **4,** 1203-1209. (e) A. M. Beatty, B. A. Helfrich, G. A. Hogan, B. A. Reed, *Cryst. Growth Des.,* 2006, **6,** 122-125. (f) C.-L. Chen, A. M. Beatty, *J. Am. Chem. Soc.,* 2008, **130,** 17222-17223. (g) B. Das, A. K. Boudalis, J. B. Baruah, *Inorg. Chem. Commun.,* 2010, **13**, 1244-1248. (h) T. D. Keene, I. Zimmermann, A. Neels, O. Sereda, J. Hauser, S. X. Liu, S. Decurtins, *Cryst. Growth Des.,* 2010, **10,** 1854-1859. (i) B. Das, J. B. Baruah, *Cryst. Growth Des.,* 2010, **10,** 3242-3249. (j) S. Santra, B. Das, J. B. Baruah, *J. Chem. Crystallogr.,* 2011, **41,** 1981-1987. (k) B. Das, J. B. Baruah, *Inorg. Chim. Acta,* 2011, **372**, 389-393. (l) B. Das, D. C. Crans, J. B. Baruah, *Inorg. Chim. Acta* 2013, **408,** 204-208.

8. (a) M. J. Prakash, A. G. Oliver, S. C. Sevov, *Cryst. Growth Des.,* 2012, **12,** 2684-2690. (b) M. J. Prakash, S. C. Sevov, *Inorg. Chem.,* 2011, **50,** 12788-12793.

9. (a) P. Mukhopadhyay, Y. Iwashita, M. Shirakawa, S-I Kawano, N. Fujita, and S. Shinkai, *Angew. Chem. Int. Ed.* 2006, **45**, 1592-1595. (b) N. Barooah, R. J. Sarma, J. B. Baruah, *Cryst. Growth Des.* 2003, **3**, 639-641. (c) N. Barooah, R. J. Sarma, A. S. Batsanov, J. B. Baruah, *J. Mol. Struct.* 2006, **791**, 122-130. (d) N. Barooah, R. J. Sarma, J. B. Baruah, *CrystEngComm* 2006, **8**, 608-615.

10. K. Hakansson, M. Lindahl, G. Svensson, J. Albertsson, *Acta Chem. Scand.,* 1993, **47**, 449-455.

11. E. Melnic, E. B. Coropceanu, O. V. Kulikova, A. V. Siminel, D. Anderson, H. J. Rivera-Jacquez, A. E. Masunov, M. S. Fonari, V. Ch. Kravtsov, *J. Phys. Chem. C,* 2014, **118**, 30087-30100.

12. (a) H.-J. Kim, D. Moon, M. S. Lah, J. -I. Honga, *Tetrahedron Lett.,* 2003, **44**, 1887-1890. (b) R. E. Sheridan, H. W. Whitlock, Jr., *J. Am. Chem. Soc.,* 1988, **110,** 4071-4073. (c) B. J. Whitlock, H. W. Whitlock, *J. Am. Chem. Soc.,* 1990, **110,** 3910-3915. (d) R. P. Sijbesma, A. P. M. Kentgens, E. T. G. Lutz, J. H. van der Maas, R. J. M. Nolte, *J. Am. Chem. Soc.,* 1993, **115,** 8999-9005. (e) G. T. W. Gieling, H. W. Scheeren, R. Israel, R. J. M. Nolte, *Chem. Commun.,* 1996, 241-243. (f) N. Barooah, J. B. Baruah, *J. Mol. Struct.,* 2008, **872,** 205-211. (g) N. Barooah, R. J. Sarma, J. B. Baruah, *CrystEngComm,* 2006, **8**, 608-615. (h) N. Barooah, R. J. Sarma, J. B. Baruah, *Cryst. Growth Des.,* 2003, **3**, 639-641.

13. (a) R. Rebek, Jr. *Angew. Chem. Int. Ed.,* 1990, **29,** 245-255. (b) S. Goswami, A. D. Hamilton, D. J. van Engen, *J. Am. Chem. Soc.,* 1989, **111**, 3425-3426.

14. (a) S. C. Zimmerman, W. Wu, *J. Am. Chem. Soc.,* 1989, **111**, 8054-8055. (b) S. C. Zimmerman, C. M. van Zyl, *J. Am. Chem. Soc.,* 1987, **109,** 7894-7896. (c) M. Harmata, C. L. Barnes, *J. Am. Chem. Soc.,* 1990, **112,** 5655-5657. (d) F. Diederich, S. B. Ferguson, *Angew. Chem. Int. Ed.,* 1986, **25,** 1127-1129. (e) R. E. Sheridan, H. W. Whitlock, Jr., J. Am. Chem. Soc., 1986, **108,** 7120-7121. (f) B. Escuder, J. F. Miravet, J. A. Saez, *Org. Biomol. Chem.,* 2008, **8,** 4378-4383. (g) W. Guan, J. Pan, X. Wang, W. Hu, L. Xu, X. Zou, C. Li, *J. Separation Sci.,* 2011, **34**, 1244-1252. (h) G. Xu, L. Yang, M. Zhong, C. Li, X. Lu, X. Kan, *Microchim. Acta,* 2013, **180,** 1461-1469. (i) C. Rosler, R. A. Fischer, *CrystEngComm,* 2015, **17**, 199-217.

15. R. Kusaka, Y. Inokuchi, T. Haino, T. Ebata, *J. Phys. Chem. Lett.*, 2012, **3**, 1414-1420.

16. R. P. Sijbesma A. P. M. Kentgens, E. T. G. Lutz, J. H. van der Maas, R. J. M. Nolte, *J. Am. Chem. Soc.,* 1993, **115**, 8999-9005.

17. (a) B. M. Holligan, J. C. Jeffery, M. D. Ward, *J. Chem. Soc. Dalton Trans.* 1992, 3337-3344. (b) J. Rubin, G. S. Panson, *J. Phys. Chem.* 1965, **69**, 3089-3091.

18. (a) D. B. Amabilino, J. F. Stoddart, *Chem. Rev.* 1995, **95**, 2725-2828. (b) L. Fang, M. A. Olson, D. Benitez, E. Tkatchouk, W. A. Goddard, J. F. Stoddart, *Chem. Soc. Rev.* 2010, **39**,17-29.

19. (a) V. A. Blatov, *IUCr CompComm Newsletter*, 2006, **7**, 4-38. (b) V. A. Blatov, A. P. Shevchenko, D. M. Proserpio, *Cryst. Growth Des.*, 2014, **14**, 3576-3586. (c) E. V. Peresypkina, V. A. Blatov, *Acta Cryst.*, 2000, **B56**, 1035-1045.

20. L. Infantes, S. Motherwell, *CrystEngComm*, 2002, **4**, 454-461.

21. (a) M. V. Kirillov, A. M. Kirillova, M. F. C. G. da Silva, M. N. Kopylovich, J. J. R. Frausto da Silva, A. J. L. Pombeiro, *Inorg. Chim. Acta*, 2008, **361**, 1728-1737. (b) F. H. Allen, *Acta Crystallogr.*, 2002, **B58**, 380-388.

22. G. M. Sheldrick *Acta Crystallogr.* 2008, **A64**, 112-122.

Supplementary Information:

A modular approach for molecular recognition by zinc dipicolinate complexes

Krapa Shankar, Alexander M. Kirillov and Jubaraj B. Baruah

List of supporting information:

Figure 1S: ^{1}H-NMR spectra (DMSO-d_6) of 1,3-bis(4-pyridine)propane, 2,7-dihydroxynaphthalene, mixture of 1,3-bis(4-pyridine)propane and 1,3-bis(4-pyridine)propane, and complex **4**.

Figure 2S: ^{1}H-NMR (DMSO-d_6) spectra of (i) 4,4′-bipyridine, (ii) 2,7-dihydroxynaphthalene, (iii) 1:1 mixture of 4,4′-bipyridine and 2,7-dihydroxynaphthalene, and (iv) complex **5**.

Figure 3S: ^{1}H-NMR spectra(DMSO-d_6) of 4,4′-bipyridine, pyrogallol, mixture of 4,4′-bipyridine and pyrogallol, and complex **6**.

Figure 4S: ^{1}H-NMR spectra (DMSO-d_6) of 1,3-bis(4-pyridine)propane, 2,6-dihydroxynaphthalene, mixture of 1,3-bis(4-pyridine)propane and 2,6-dihydroxynaphthalene, and complex **7**.

Figure 5S: Thermogram of Complex **1**

Figure 6S: Thermogram of Complex **2**

Figure 7S: Thermogram of Complex **3**

Figure 8S: Thermogram of Complex **4**

Figure 9S: Thermogram of Complex **5**

Figure 10S: Thermogram of Complex **6**

Figure 11S: Thermogram of Complex **7**

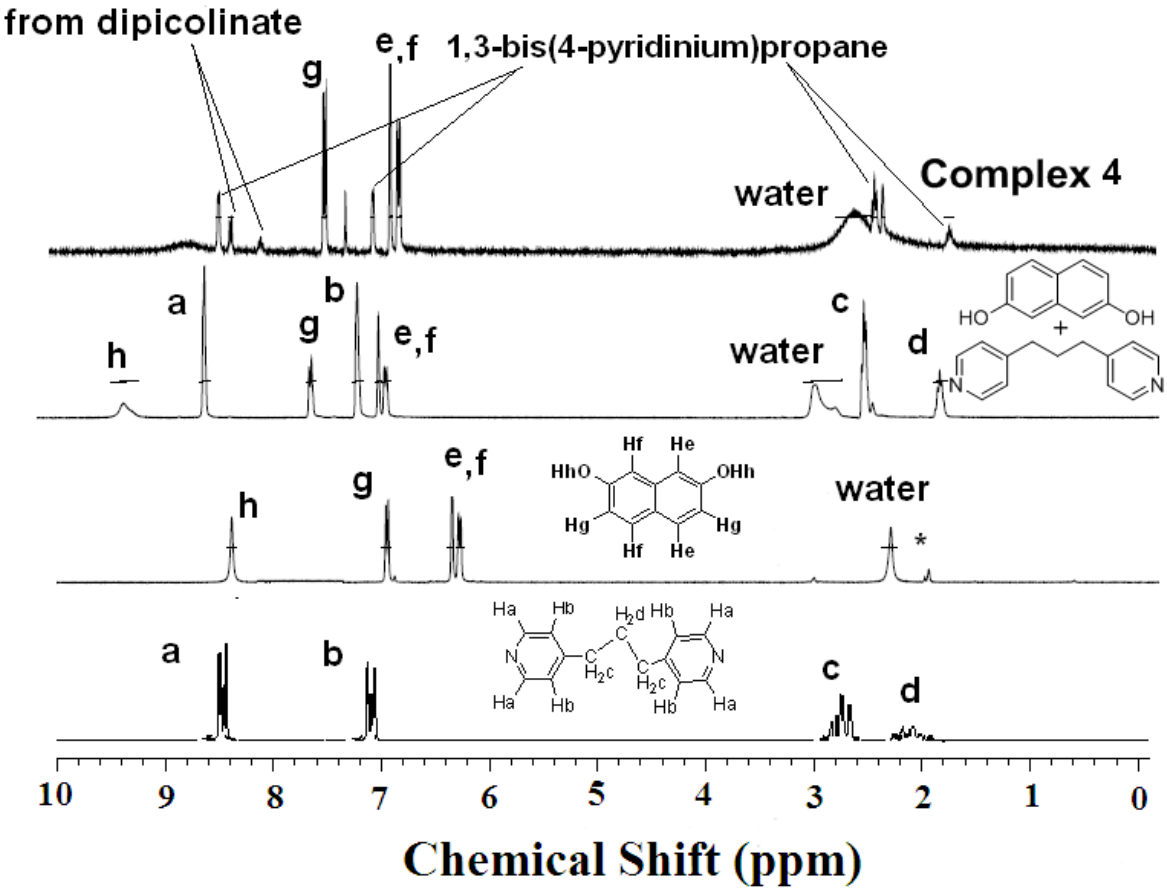

Figure 1S: ^{1}H-NMR spectra (DMSO-d_6) of 1,3-bis(4-pyridine)propane, 2,7-dihydroxynaphthalene, mixture of 1,3-bis(4-pyridine)propane and 1,3-bis(4-pyridine)propane, and complex **4**.

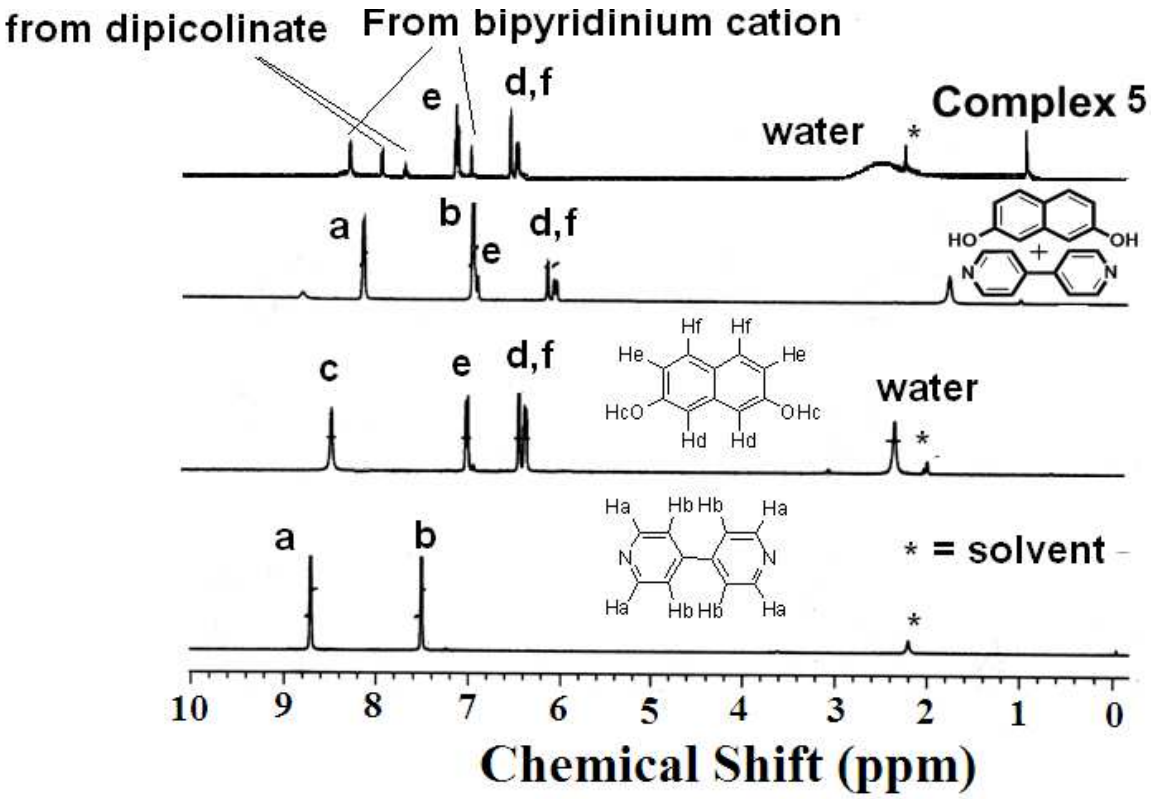

Figure 2S: ^{1}H-NMR (DMSO-d_6) spectra of (i) 4,4′-bipyridine, (ii) 2,7-dihydroxynaphthalene, (iii) 1:1 mixture of 4,4′-bipyridine and 2,7-dihydroxynaphthalene, and (iv) complex **5**.

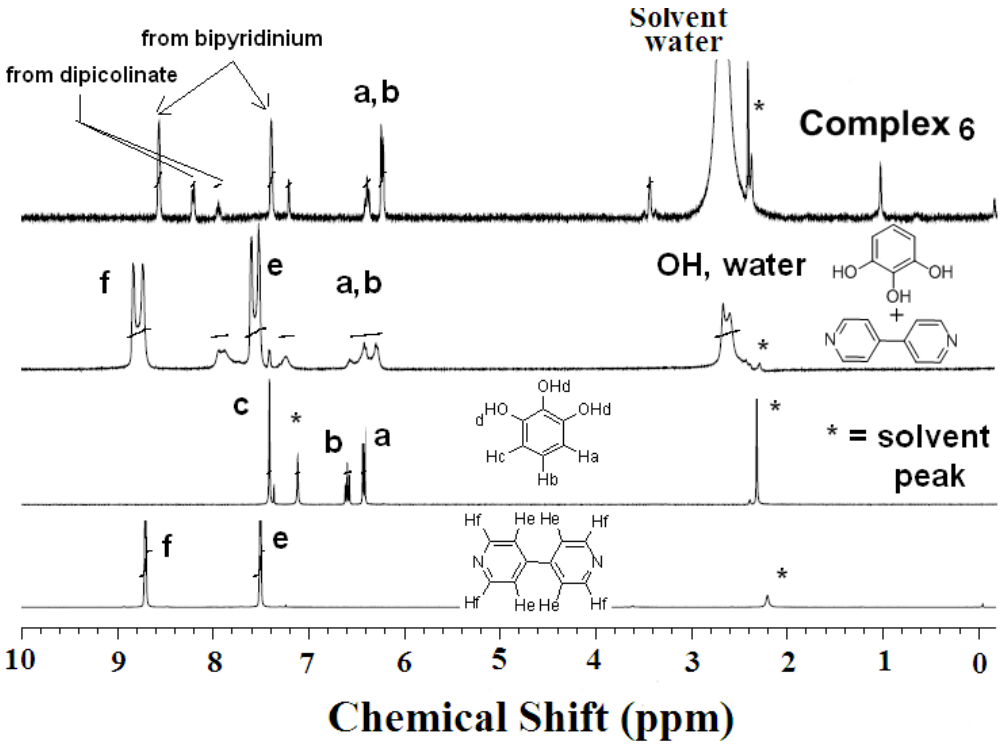

Figure 3S: ^{1}H-NMR spectra (DMSO-d_6) of 4,4′-bipyridine, pyrogallol, mixture of 4,4′-bipyridine and pyrogallol, and complex **6**.

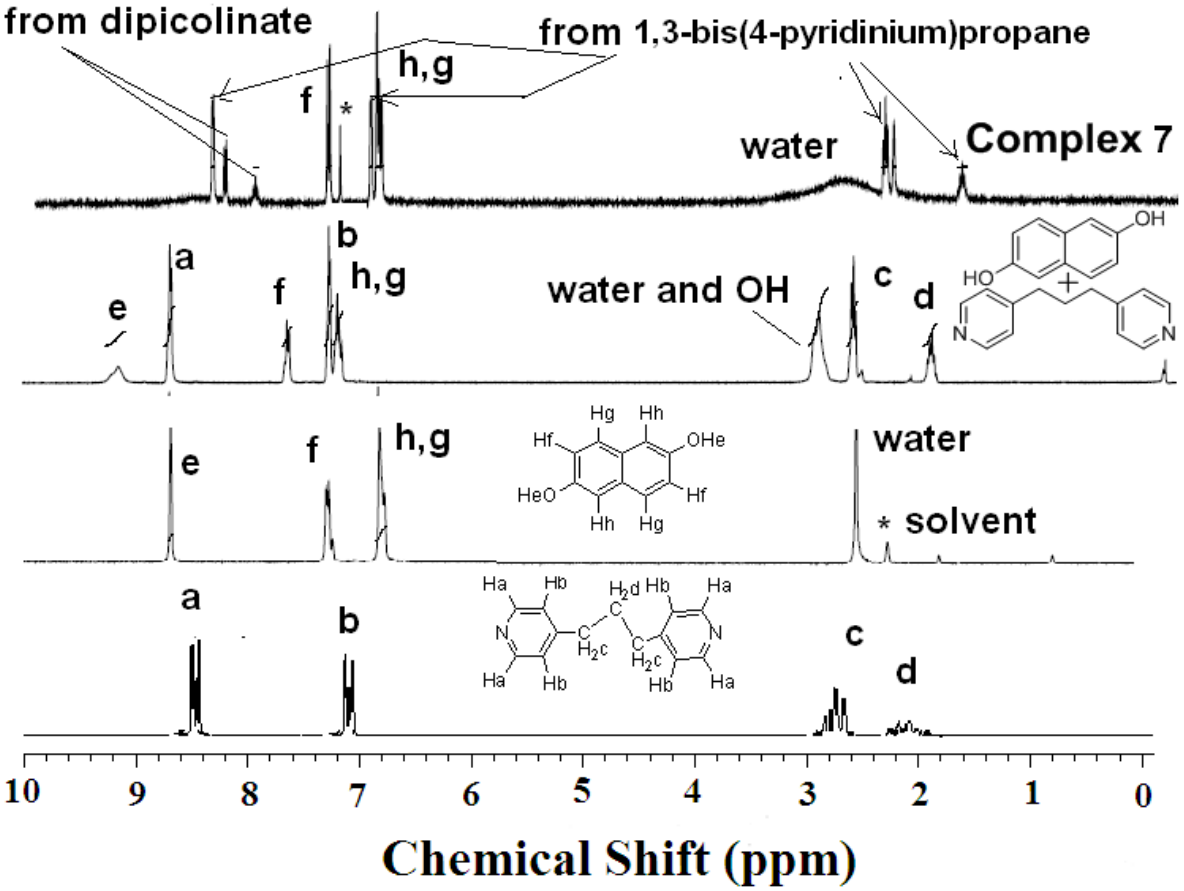

Figure 4S: ^{1}H-NMR spectra(DMSO-d_6) of 1,3-bis(4-pyridine)propane, 2,6-dihydroxynaphthalene, mixture of 1,3-bis(4-pyridine)propane and 2,6-dihydroxynaphthalene, and complex **7**.

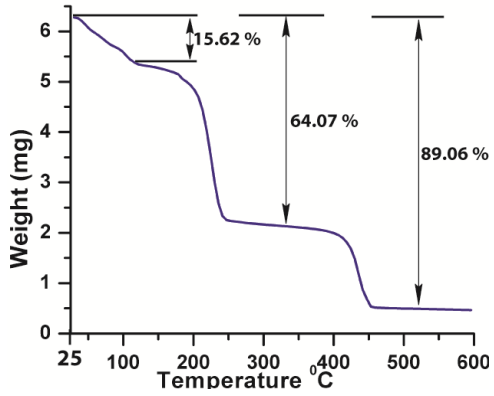

Figure 5S: Thermogram of complex **1**

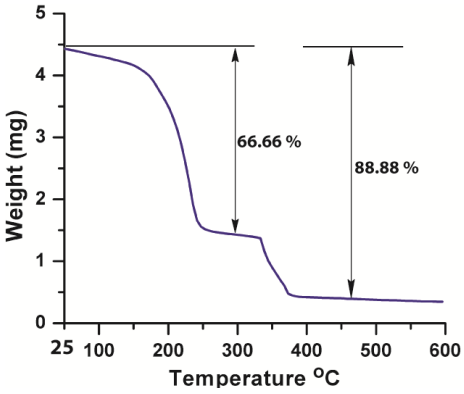

Figure 6S: Thermogram of complex **2**

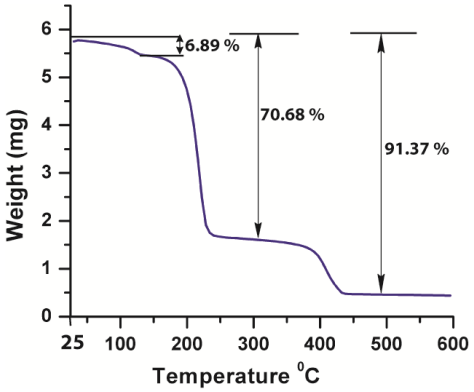

Figure 7S: Thermogram of complex **3**

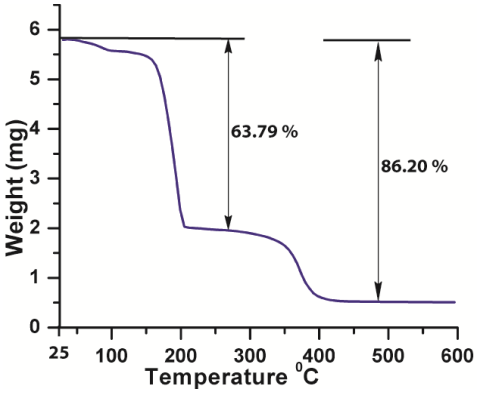

Figure 8S: Thermogram of complex **4**

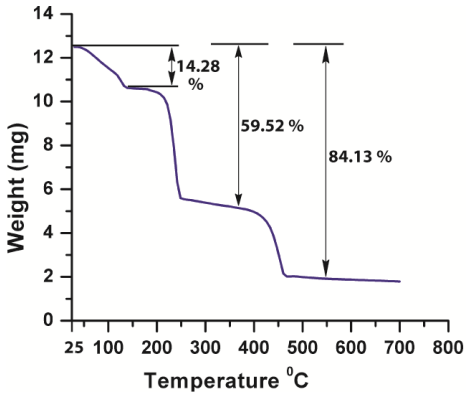

Figure 9S: Thermogram of complex **5**

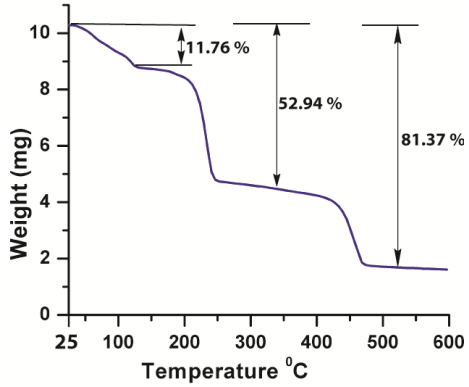

Figure 10S: Thermogram of complex **6**

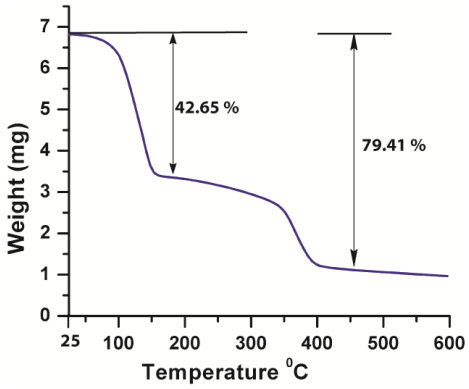

Figure 11S: Thermogram of complex **7**